

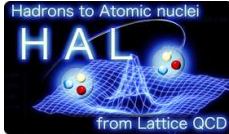
Central and tensor Lambda-Nucleon potentials from lattice QCD

Hidekatsu Nemura*

Department of Physics, Tohoku University, Sendai, 980-8578, Japan

E-mail: nemura@nucl.phys.tohoku.ac.jp

for HAL QCD and PACS-CS Collaboration



We present our latest study of Lambda-Nucleon (ΛN) interaction by using lattice QCD, following up on our report at LATTICE 2008. We have calculated not only the scattering lengths but also the central and tensor potentials, which are obtained from the Bethe-Salpeter (BS) amplitude measured in lattice QCD. For these calculations, we employ two different types of gauge configurations: (i) 2+1 flavor full QCD configurations generated by the PACS-CS collaboration at $\beta = 1.9$ ($a = 0.0907(13)$ fm) on a $32^3 \times 64$ lattice, whose spatial volume is $(2.90 \text{ fm})^3$, with the quark masses corresponding to $(m_\pi, m_K) \approx (301, 592)$, $(414, 637)$, $(570, 724)$ and $(699, 787)$ (in units of MeV). (ii) Quenched QCD configurations at $\beta = 5.7$ ($a = 0.1416(9)$ fm) on a $32^3 \times 48$ lattice, whose spatial volume is $(4.5 \text{ fm})^3$, with the quark masses corresponding to $(m_\pi, m_K) \approx (512, 606)$, $(464, 586)$ and $(407, 565)$. The following qualitative features are found: The Λp potential has a relatively strong (weak) repulsive core in the 1S_0 (3S_1) channel at short distance, while the potential has slight attractive region at medium distance. The tensor potential is found to be weaker than the NN case. These results hold in both full and quenched QCD. The energy of the ground state on the finite lattice volume is calculated: In both spin channels, energy shift due to the finite volume, from which we extract the scattering length via the Lüscher's formula, is found to be negative at all values of quark masses, suggesting that the ΛN interaction is attractive. We have also discussed the quark mass dependences of the potentials and the scattering lengths.

The XXVII International Symposium on Lattice Field Theory - LAT2009

July 26-31 2009

Peking University, Beijing, China

*Speaker.

1. Introduction

The hyperon-nucleon (YN) and the hyperon-hyperon (YY) interactions are the keys to explore the strange nuclear systems, in which hyperons (or strange quarks) are embedded in normal nuclear systems as “impurities” [1]. For example, spectroscopic studies of the Λ and Σ hypernuclei are carried out experimentally and theoretically, which leads to a qualitative conclusion that the Λ -nucleus interaction is attractive while the Σ -nucleus interaction is repulsive. Such information is useful to study the composition of hyperonic matter inside the neutron stars [2]: the Λ particle instead of Σ^- would be the first strange baryon to appear in the core of the neutron stars. The ΞN interaction is also interesting and important, in order to explore the existence of Ξ hypernuclei and the dense hyperonic matter in neutron stars. Despite their importance, YN and YY interactions have still large uncertainties because direct YN and YY scattering experiments are either difficult or impossible due to the short life-time of hyperons.

Under these circumstances, the lattice QCD would be a valuable theoretical tool to make a first-principle calculation of baryon-baryon interactions. Previously, scattering parameters based on the Lüscher’s formula have been reported for the NN system [4, 5] and for the YN system [6, 7]. Recently, a new approach to the NN interaction from the lattice QCD has been proposed [8]. In this approach, the NN potential can be directly obtained from lattice QCD through the Bethe-Salpeter (BS) amplitude and the observables such as the phase shift and the binding energy can be calculated by using the resultant potential. See Refs. [9, 10, 11, 12, 13, 14] for the recent developments in various aspects along the line of this approach.

The purpose of this report is to present our recent calculation of the ΛN potentials together with the scattering parameters by using the full and quenched QCD gauge configurations. A preliminary result was already reported at LATTICE 2008[15]. This is the latest version of the report which includes several new efforts: (i) Not only the central potential but also the tensor potential are calculated, (ii) quark mass dependences of the potentials and the scattering lengths are studied, and (iii) statistics of the lattice are increased from the previous report.

2. Formulation

The basic formulation has already been given in Refs. [8, 11, 16, 17]. (See also Refs. [3, 18].) and a recent comprehensive accounts for the lattice NN potential is found in [14]. The formulation for the YN interaction is reported in [15], so that we mention only the basic equations briefly below. We start from an effective Schrödinger equation for the equal-time BS wave function:

$$-\frac{1}{2\mu}\nabla^2\phi(\vec{r}) + \int U(\vec{r},\vec{r}')\phi(\vec{r}')d^3r' = E\phi(\vec{r}). \quad (2.1)$$

Here $\mu = m_\Lambda m_N / (m_\Lambda + m_N)$ and $E \equiv k^2 / (2\mu)$ are the reduced mass of the ΛN system and the non-relativistic energy in the center-of-mass frame, respectively. We consider the low-energy scattering state so that the nonlocal potential can be rewritten by the derivative or velocity expansion [19], $U(\vec{r},\vec{r}') = V_{\Lambda N}(\vec{r},\vec{\nabla})\delta(\vec{r}-\vec{r}')$. The general expression of the potential $V_{\Lambda N}$ is known to be [20]

$$V_{\Lambda N} = V_0(r) + V_\sigma(r)(\vec{\sigma}_\Lambda \cdot \vec{\sigma}_N) + V_T(r)S_{12} + V_{LS}(r)(\vec{L} \cdot \vec{S}_+) + V_{ALS}(r)(\vec{L} \cdot \vec{S}_-) + O(\nabla^2). \quad (2.2)$$

Here $S_{12} = 3(\vec{\sigma}_\Lambda \cdot \vec{n})(\vec{\sigma}_N \cdot \vec{n}) - \vec{\sigma}_\Lambda \cdot \vec{\sigma}_N$ is the tensor operator with $\vec{n} = \vec{r}/|\vec{r}|$, $\vec{S}_\pm = (\vec{\sigma}_N \pm \vec{\sigma}_\Lambda)/2$ are symmetric (+) and antisymmetric (−) spin operators, $\vec{L} = -i\vec{r} \times \vec{\nabla}$ is the orbital angular momentum operator. $V_{0,\sigma,T}$ are the leading order (LO) potentials while $V_{LS,ALS}$ are the next-to-leading-order (NLO) potentials in the velocity expansion. The procedure to derive the LO potentials is as follows. For the spin triplet state, the noncentral forces (e.g. the tensor force) mix different partial waves such as S - and D -waves. Namely, the spin-triplet wave function $\phi(r; J=1)$ comprises the S - and the D -wave components, which can be extracted from the lattice wave function $\phi_{\alpha\beta}(r; J=1)$ such that (See [15] for the method to obtain $\phi_{\alpha\beta}(r; J)$ in lattice QCD.)

$$\begin{cases} \phi_{\alpha\beta}(r; {}^3S_1) = \mathcal{P}\phi_{\alpha\beta}(r; J=1) \equiv \frac{1}{24} \sum_{\mathcal{R} \in O} \mathcal{R}\phi_{\alpha\beta}(r; J=1), \\ \phi_{\alpha\beta}(r; {}^3D_1) = \mathcal{Q}\phi_{\alpha\beta}(r; J=1) \equiv (1 - \mathcal{P})\phi_{\alpha\beta}(r; J=1). \end{cases} \quad (2.3)$$

Therefore, the effective Schrödinger equation with the LO potentials becomes:

$$\begin{Bmatrix} \mathcal{P} \\ \mathcal{Q} \end{Bmatrix} \times \left\{ -\frac{1}{2\mu} \nabla^2 + V_0(r) + V_\sigma(r)(\vec{\sigma}_\Lambda \cdot \vec{\sigma}_N) + V_T(r)S_{12} \right\} \phi(\vec{r}) = \begin{Bmatrix} \mathcal{P} \\ \mathcal{Q} \end{Bmatrix} \times E\phi(\vec{r}) \quad (2.4)$$

The r dependence of the central and the tensor potentials, $V_C(r; J=0) = V_0(r) - 3V_\sigma(r)$ for $J=0$, $V_C(r; J=1) = V_0(r) + V_\sigma(r)$, and $V_T(r)$ for $J=1$, are determined once we obtain the wave function, the total energy and the reduced mass in lattice QCD.

3. Numerical simulations

3.1 2+1 flavor QCD

Main results in this report are obtained by using the 2+1 flavor full QCD gauge configurations generated by PACS-CS collaboration [21] with the RG-improved Iwasaki gauge action and the non-perturbatively $O(a)$ -improved Wilson quark action at $\beta = 1.9$ on a $32^3 \times 64$ lattice. The lattice spacing at the physical quark masses has been estimated as $a = 0.0907(13)$ fm [21]. So far, we have employed four values of the hopping parameter for light quarks, $\kappa_{ud} = 0.13700, 0.13727, 0.13754, 0.13770$, while the one for the strange quark is fixed to $\kappa_s = 0.13640$. Several light hadron masses obtained in the present calculation are shown in Table 1. To calculate the BS wave function, the wall source is placed at the time-slice t_0 with the Coulomb gauge fixing, and the Dirichlet boundary condition is imposed in the temporal direction at the time-slice $t - t_0 = 32$. In order to improve the statistics, multiple sources at $t_0 = 8n$ with $n = 0, 1, 2, \dots, 8$ are employed on each gauge configuration. The results are obtained with $N_{\text{conf}} = 609, 481, 568, 422$ for $\kappa_{ud} = 0.13700, 0.13727, 0.13754, 0.13770$, respectively, where N_{conf} is the number of the gauge configurations.

3.2 Quenched QCD with larger spatial volume

In quenched QCD calculation, we employ the plaquette gauge action and the Wilson quark action at $\beta = 5.7$ on a $32^3 \times 48$ lattice. The periodic boundary condition is imposed for quarks in the spatial direction. The wall source is placed at $t_0 = 0$ with the Coulomb gauge fixing and the Dirichlet boundary condition is imposed at $t = 24$ in the temporal direction. The lattice spacing at the physical point is determined as $a = 0.1416(9)$ fm ($1/a = 1.393(9)$ GeV) from $m_\rho = 770$ MeV. The spatial lattice volume is $(4.5\text{fm})^3$. The hopping parameter for the strange quark mass

is given by $\kappa_s = 0.16432(6)$ from $m_K = 494$ MeV. Three values of the hopping parameter, $\kappa_{ud} = 0.1665, 0.1670, 0.1675$, are employed for the light quark mass. Table 1 also lists the light hadron masses calculated in quenched QCD. The results in quenched QCD are obtained with $N_{\text{conf}} \approx 1000$.

4. Numerical results

4.1 2+1 flavor QCD

Figures 1 and 2 show the ΛN potentials obtained from 2+1 flavor QCD calculation as a function of r . The central ($V_C(J=1)$) and the tensor (V_T) potentials in the ${}^3S_1 - {}^3D_1$ channels are given in Fig. 1 while the central potential in the 1S_0 channel ($V_C(J=0)$) is given in Fig. 2. We also show the central potential multiplied by volume factor ($r^2 V_C(r)$) in the left panel in addition to the normal $V(r)$ given in the right panel, in order to compare the strength of the repulsive force between two quark masses. These figures contain results with $(m_\pi, m_K) \approx (699, 787)$ and $(414, 637)$ MeV, which are obtained at $t - t_0 = 13$ and 10 , respectively. These time-slices are chosen so that the ground state saturation is achieved.

As can be seen in both figures, the attractive well of the central potential moves to outer region as the u, d quark mass decreases while the depth of these attractive pockets do not change so much. The present results show that the tensor force is weaker than the NN case [17], and the quark mass dependence of the tensor force seems to be small. Both of the repulsive and attractive parts increase in magnitude as the u, d quark mass decreases.

For $m_\pi \approx 700$ MeV, the central potentials reach $V_C \rightarrow 0$ at the radial distance $r \sim 1.3$ fm, which is smaller than the half of the physical lattice length ($aL/2 \approx 1.45$ fm). Therefore the Lüscher's formula can be applied to extract the scattering phase shift, which will be discussed in the latter subsection. For $m_\pi \approx 400$ MeV, on the other hand, the interaction range of the V_C , which is about 1.4 fm, almost reaches to the half of the lattice. Therefore we must be very careful to extract the scattering phase shift at this or lighter quark masses from the Lüscher's formula, though no sign of the violation against the Lüscher's condition was observed within errors for the effective central potential even at $m_\pi \approx 300$ MeV. (See Fig. 1 in the previous report [15].) Calculation on larger spatial volume will be needed to correctly extract the scattering phase shift at $m_\pi \approx 300$ MeV.

κ_{ud}	m_π	m_ρ	m_K	m_{K^*}	m_N	m_Λ	m_Σ	m_Ξ
2+1 flavor QCD by PACS-CS with $\kappa_s = 0.13640$								
0.13700	699.4(4)	1108(3)	786.8(4)	1159(2)	1572(6)	1632(4)	1650(5)	1701(4)
0.13727	567.9(6)	1000(4)	723.7(7)	1081(3)	1396(6)	1491(4)	1519(5)	1599(4)
0.13754	413.6(6)	902(3)	636.6(4)	1026(3)	1221(7)	1349(4)	1406(8)	1505(4)
0.13770	301(3)	845(10)	592(1)	980(6)	1079(12)	1248(15)	1308(13)	1432(7)
quenched QCD with $\beta = 5.7, \kappa_s = 0.1643$								
0.1665	511.8(5)	862(3)	605.8(5)	898(1)	1297(6)	1344(6)	1375(5)	1416(3)
0.1670	463.6(6)	842(4)	586.3(5)	895(2)	1250(9)	1314(9)	1351(6)	1404(4)
0.1675	407(1)	820(3)	564.9(5)	886(3)	1205(13)	1269(9)	1326(9)	1383(5)
Exp.	135	770	494	892	940	1116	1190	1320

Table 1: Hadron masses in the unit of MeV.

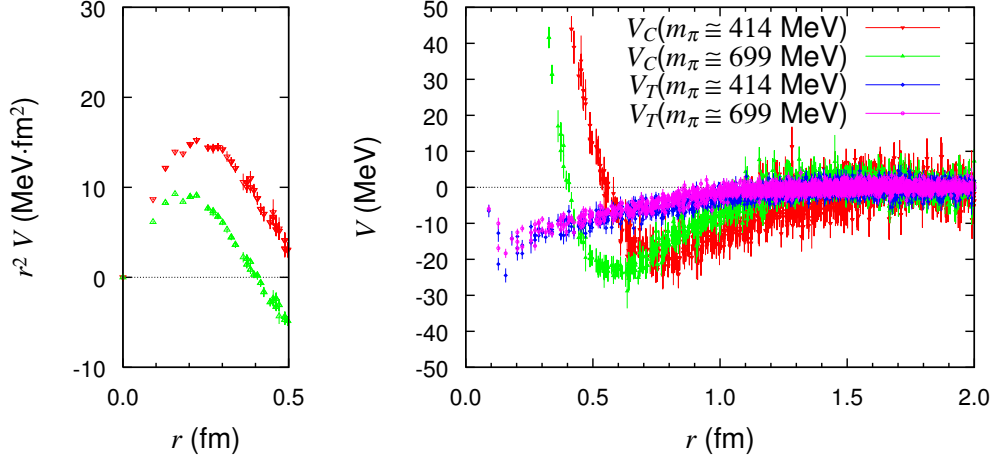


Figure 1: The central and the tensor potentials in ${}^3S_1 - {}^3D_1$ channel in 2 + 1 flavor QCD as a function of r at $m_\pi \simeq 414$ MeV (red and blue) and 699 MeV (green and magenta).

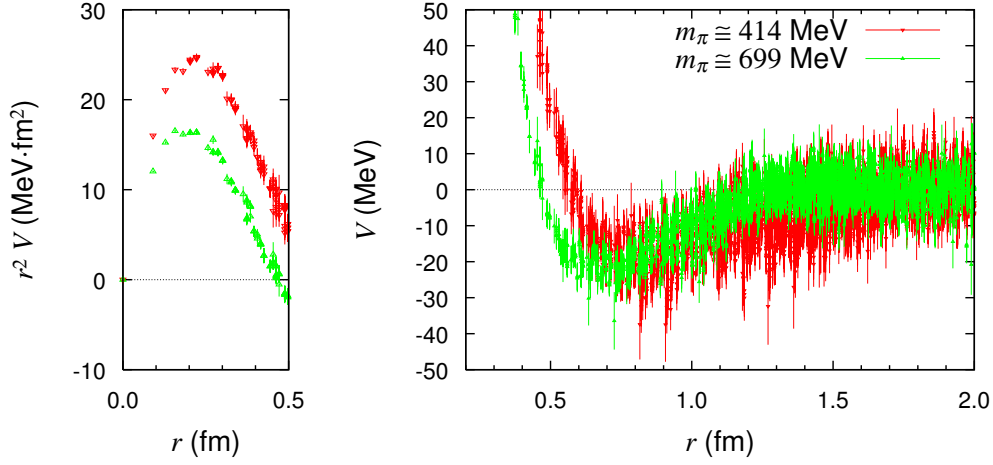


Figure 2: The central potential in 1S_0 channel in 2 + 1 flavor QCD as a function of r at $m_\pi \simeq 414$ MeV (red) and 699 MeV (green).

4.2 Quenched QCD

Figures 3 and 4 show the ΛN potentials with $(m_\pi, m_K) \approx (512, 606)$ and $(407, 565)$ MeV, in quenched QCD at the time-slice $t - t_0 = 7$. Fig. 3 shows the $V_C(J = 1)$ and V_T , while the Fig. 4 shows the $V_C(J = 0)$. We find that the qualitative behaviors of the ΛN potential in quenched QCD are more or less similar to those in full QCD in both $J = 1$ and 0 channels: Namely, the attractive pocket of the central potential moves to longer distance region as the quark mass decreases, and the quark mass dependence of the tensor potential seems to be small.

4.3 Scattering lengths

Figure 5 shows the scattering lengths as a function of m_π^2 , which are calculated through the

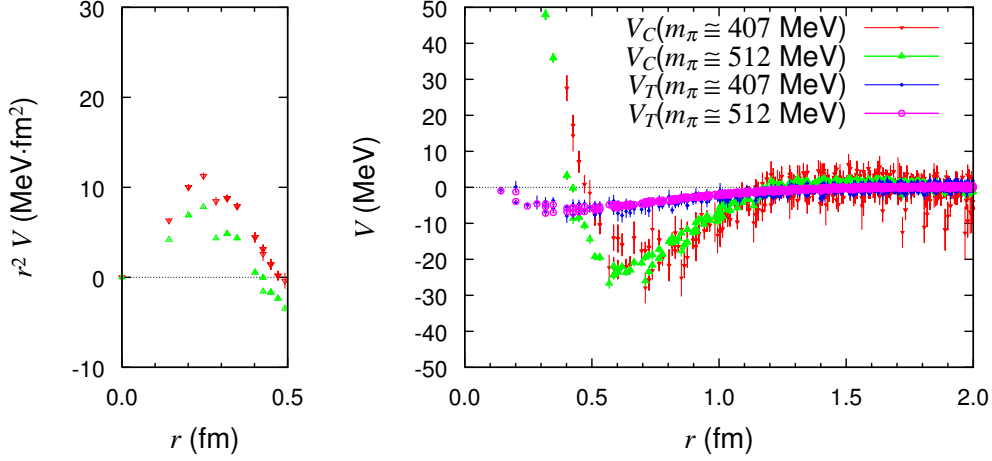


Figure 3: The central and the tensor potentials in ${}^3S_1 - {}^3D_1$ channel in quenched QCD at $m_\pi \simeq 407$ MeV (red and blue) and 512 MeV (green and magenta).

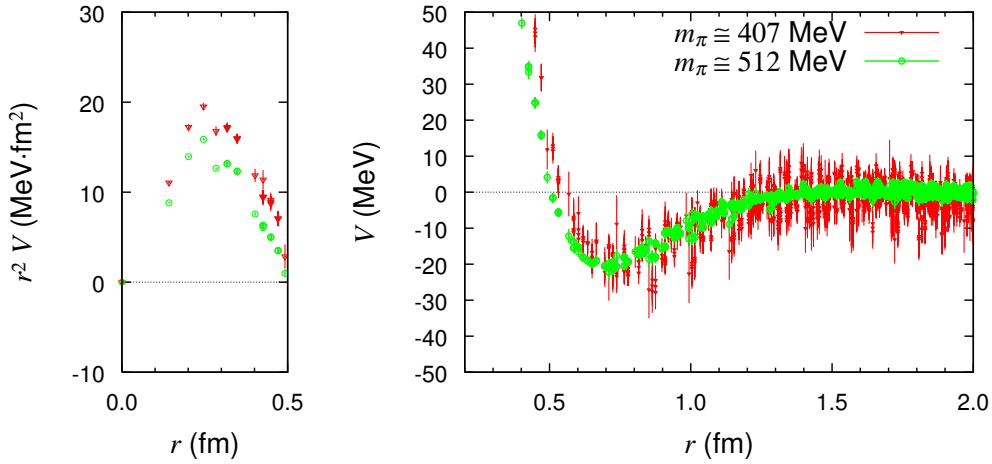


Figure 4: The central potential in 1S_0 channel in quenched QCD at $m_\pi \simeq 407$ MeV (red) and 512 MeV (green).

Lüscher's formula [3, 18]

$$k \cot \delta_0(k) = \frac{2}{\sqrt{\pi}L} Z_{00}(1; (kL/(2\pi))^2) = 1/a_0 + O(k^2),$$

$$\text{with } Z_{00}(s; q^2) = \frac{1}{\sqrt{4\pi}} \sum_{\vec{n} \in Z^3} (n^2 - q^2)^{-s} \quad (\text{Re } s > 3/2),$$
(4.1)

where $Z_{00}(1; q^2)$ is obtained by the analytic continuation in s . The energy, $E = \frac{k^2}{2\mu}$, on the finite lattice volume is determined by fitting the asymptotic region of the BS wave function in terms of the Green's function

$$G(\vec{r}, k^2) = \frac{1}{L^3} \sum_{\vec{p} \in \Gamma} \frac{1}{p^2 - k^2} e^{i\vec{p} \cdot \vec{r}}, \quad \Gamma = \left\{ \vec{p}, \vec{p} = \vec{n} \frac{2\pi}{L}, \vec{n} \in Z^3 \right\},$$
(4.2)

which is the solution to the Helmholtz equation $(\Delta + k^2)G(\vec{r}, k^2) = -\delta_L(\vec{r})$ with $\delta_L(\vec{r})$ being the periodic delta function[3, 18].

As is seen in the Fig. 5, the scattering lengths are almost constant for larger u, d quark mass corresponding to $m_\pi \gtrsim 560$ MeV. On the other hand, for lighter u, d quark mass region that 400 MeV $\lesssim m_\pi \lesssim 500$ MeV, the present result seems to show that the scattering lengths increase as the u, d quark mass decreases. The present values are still much smaller than the empirical scattering lengths of ΛN , $a_0 \sim 1.5 - 2.5$ fm, estimated from the measurement of the ΛN total cross section and the theoretical studies of Λ -hypernuclei. The scattering lengths calculated in quenched QCD are qualitatively similar to those in $2 + 1$ flavor QCD. As is discussed in the former subsection, we will need larger spatial volume in full QCD to extract the scattering lengths reliably at $m_\pi \lesssim 300$ MeV.

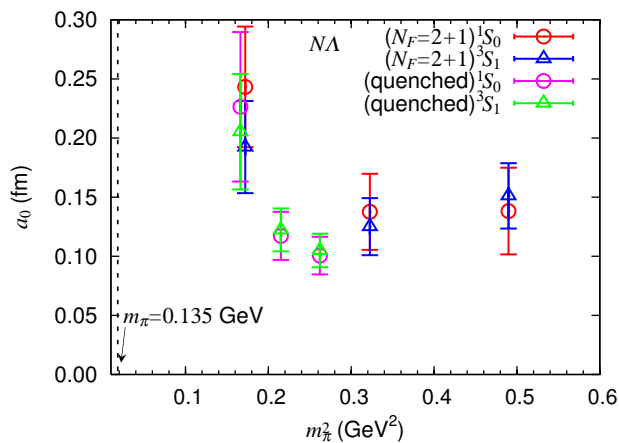


Figure 5: Scattering lengths of ΛN interaction as a function of m_π^2 .

5. Summary

We have calculated the central and tensor parts of ΛN potentials as well as the scattering lengths in lattice QCD at several values of the u, d quark mass corresponding to $m_\pi \simeq 300 - 700$ MeV. The central potentials indicate that the interaction range becomes larger while the depth of the attractive well hardly changes as the u, d quark mass decreases. On the other hand the tensor force has relatively a weak quark mass dependence. The present result of the scattering lengths shows that the ΛN interaction is attractive and becomes stronger as the u, d quark mass decreases. The calculation in $2 + 1$ full QCD for the ΛN system with larger volume and smaller lattice spacing at physical quark mass is highly desirable for definite conclusions on the nature of the ΛN interaction.

Acknowledgments

The authors would like to thank PACS-CS Collaboration for allowing us to access their full QCD gauge configurations, and Dr. T. Izubuchi for providing a sample FFT code. The full QCD calculations have been done by using PACS-CS computer under the “Interdisciplinary Computational Science Program” of Center for Computational Science, University of Tsukuba (No 09a-11). The quenched QCD calculations have been done by using Blue Gene/L computer under the “Large

scale simulation program” at KEK (No. 09-23). H.N. would also like to thank Dr. K. Itahashi and Advanced Meson Science Laboratory of RIKEN Nishina Center for providing a special computer resource. H. N. is supported by the Global COE Program for Young Researchers at Tohoku University (No. 22210005). This research was partly supported by the MEXT Grant-in-Aid, Scientific Research on Priority Areas (No. 20028013) and Scientific Research on Innovative Areas (Nos. 21105515, 20105003).

References

- [1] Reviewed in O. Hashimoto and H. Tamura, *Prog. Part. Nucl. Phys.* **57**, 564 (2006).
- [2] See e.g. J. Schaffner-Bielich, *Nucl. Phys. A* **804**, 309 (2008) [arXiv:0801.3791 [astro-ph]].
- [3] M. Lüscher, *Nucl. Phys. B* **354**, 531 (1991).
- [4] M. Fukugita, Y. Kuramashi, M. Okawa, H. Mino and A. Ukawa, *Phys. Rev. D* **52**, 3003 (1995) [arXiv:hep-lat/9501024].
- [5] S. R. Beane, P. F. Bedaque, K. Orginos and M. J. Savage, *Phys. Rev. Lett.* **97**, 012001 (2006) [arXiv:hep-lat/0602010].
- [6] S. Muroya, A. Nakamura and J. Nagata, *Nucl. Phys. Proc. Suppl.* **129**, 239 (2004).
- [7] S. R. Beane *et al.* [NPLQCD Collab.], *Nucl. Phys. A* **794**, 62 (2007).
- [8] N. Ishii, S. Aoki, T. Hatsuda, *Phys. Rev. Lett.* **99**, 022001 (2007).
- [9] S. Aoki, J. Balog, T. Hatsuda, N. Ishii, K. Murano, H. Nemura and P. Weisz, arXiv:0812.0673 [hep-lat].
- [10] K. Murano, [for HAL QCD Collaboration], in these proceedings.
- [11] H. Nemura, N. Ishii, S. Aoki and T. Hatsuda, *Phys. Lett. B* **673**, 136 (2009) [arXiv:0806.1094 [nucl-th]].
- [12] T. Inoue, [for HAL QCD Collaboration], in these proceedings.
- [13] N. Ishii, [for HAL QCD Collaboration], in these proceedings.
- [14] S. Aoki, T. Hatsuda and N. Ishii, arXiv:0909.5585 [hep-lat].
- [15] H. Nemura, N. Ishii, S. Aoki and T. Hatsuda [PACS-CS Collaboration], arXiv:0902.1251 [hep-lat].
- [16] S. Aoki, T. Hatsuda and N. Ishii, *Comput. Sci. Dis.* **1**, 015009 (2008) [arXiv:0805.2462 [hep-ph]].
- [17] N. Ishii, S. Aoki and T. Hatsuda, arXiv:0903.5497 [hep-lat].
- [18] S. Aoki, *et al.* [CP-PACS Collab.], *Phys. Rev. D* **71**, 094504 (2005).
- [19] R. Tamagaki and W. Watari, *Prog. Theor. Phys. Suppl.* **39**, 23 (1967).
- [20] J.J.de Swart, *et al.*, *Springer Tracts in Modern Physics* **60**, 138 (1971).
- [21] S. Aoki *et al.* [PACS-CS Collaboration], *Phys.Rev.D* **79**, 034503 (2009), arXiv:0807.1661 [hep-lat].
- [22] CPS++ http://qcdoc.phys.columbia.edu/chuiwoo_index.html.